

Geminga: A Cooling Superfluid Neutron Star

Dany Page

Department of Astronomy, Columbia University
538 West 120th Street, New York, NY 10027

ABSTRACT

We compare the recent temperature estimate for Geminga with neutron star cooling models. Because of its age ($\sim 3.4 \times 10^5$ yr), Geminga is in the photon cooling era. We show that its surface temperature ($\sim 5.2 \times 10^5$ K) can be understood by both types of neutrino cooling scenarios, i.e, slow neutrino cooling by the modified Urca process or fast neutrino cooling by the direct Urca process or by some exotic matter, and thus does not allow us to discriminate between these two competing schemes. However, for both types of scenarios, agreement with the observed temperature can only be obtained if *baryon pairing is present in most, if not all, of the core of the star*. Within the slow neutrino cooling scenario, early neutrino cooling is not sufficient to explain the observed low temperature, and extensive pairing in the core is necessary to reduce the specific heat and increase the cooling rate in the present photon cooling era. Within all the fast neutrino cooling scenarios, pairing is necessary throughout the whole core to control the enormous early neutrino emission which, without pairing suppression, would result in a surface temperature at the present time much lower than observed.

We also comment on the recent temperature estimates for PSR 0656+14 and PSR 1055-52, which pertain to the same photon cooling era. If one assumes that all neutron stars undergo fast neutrino cooling, then these two objects also provide evidence for extensive baryon pairing in their core, but observational uncertainties also permit a more conservative interpretation, with slow neutrino emission and no pairing at all. We argue though that observational evidence for the slow neutrino cooling model (the “standard” model) is in fact very dim and that the interpretation of the surface temperature of all neutron stars could be done with a reasonable theoretical *a priori* within the fast neutrino cooling scenarios only. In this case, Geminga, PSR 0656+14, and PSR 1055-52 all show evidence of baryon pairing down to their very centers.

The Astrophysical Journal, in press.

Subject headings: dense matter — stars: neutron — stars: x-rays

1. INTRODUCTION

The study of the thermal evolution of young neutron stars offers the possibility of obtaining unique information about the structure of compressed cold nuclear matter. Early cooling after the supernova explosion is driven by neutrino emission, whose rate is a very sensitive function of the state of that matter. Moreover, both the neutrino cooling and the later photon cooling are strongly affected by the occurrence of pairing (*à la* BCS) of the baryonic components of the star's core. These two aspects combined result in a wide range of predicted surface temperatures and give us two handles by which to extract information about the composition and pairing state of dense matter through comparison of neutron star cooling calculations with observations of neutron stars of known ages.

Observational candidates for this purpose must have an age well below 10^6 yr since, after this, the star has exhausted its initial heat content and its (much lower) temperature depends on other mechanisms. Interstellar absorption is significant at the photon energies corresponding to the expected surface temperatures, of the order of 10^6 K or lower, and hence the star must be not too far away from us and must be in a region of low interstellar absorption. Until recently, only three neutron stars fulfilled these two criteria of relative youth and closeness, all three located within the local bubble of low interstellar matter density surrounding the Sun: PSR 0833-45 (Vela), PSR 0656+14, and PSR 1055-52. They provided the only reliable data to compare with theoretical models. Some other objects, for example PSR 0531+21 (Crab; Harnden & Seward 1984) or the neutron star in the supernova remnant 3C58 (Becker, Helfand & Szymkowiak 1982), located at farther distances have only given rough upper limits of their surface temperatures. We refer to Ögelman (1991) for a review of the pre-*ROSAT* observational situation.

With the recent demonstration by Halpern & Holt (1992) that Geminga *is* a neutron star, a new candidate is now available. The quality of the *ROSAT* data makes this one of the best cases of detection of thermal radiation from a neutron star surface to date, and the data analysis (Halpern & Ruderman 1993) is the most detailed performed so far. Geminga is one of the closest neutron stars and is located within the local interstellar bubble; Gehrels & Chen (1993) recently argued that the Geminga supernova may have actually been the cause of this bubble.

Comparison of Geminga's age and temperature with published models of neutron star cooling shows that the data can be accommodated by a variety of models. Several of the direct Urca cooling scenarios of Page & Applegate (1992), the kaon condensate cooling scenario of Page & Baron (1990), and some of the pion condensate cooling scenarios of Umeda *et al.* (1992) work, while none of the fast cooling models, either with quarks or pion

condensate, of Van Riper (1991) is successful. Some, but not all, of the “standard” cooling models presented by Nomoto & Tsuruta (1986, 1987), Shibazaki & Lamb (1989), Page & Baron (1990), Van Riper (1991), Page & Applegate (1992), and Umeda *et al.* (1992, 1993) are also successful. In this paper, we will look at the various ingredients of these models and determine which ones are crucial for compatibility with this new neutron star. A preliminary version of this work has been presented in Page (1992).

The pulsars PSR 0656+14 and PSR 1055-52 have ages similar to Geminga’s and fit into the study of the present work. Since the analyses of the *ROSAT* observations of these two objects have been published recently (Finley, Ögelman & Kiziloğlu 1992; Ögelman & Finley 1993) we will also discuss them briefly.

The structure of the paper is as follow. Section 2 presents the observational data on Geminga. Section 3 describes the general physics of neutron star cooling relevant to our present purpose. Section 4 discusses the various fast neutrino cooling scenarios, and section 5 presents detailed calculations within the slow neutrino cooling scenario. Comparison with Geminga is done in sections 4 and 5 while section 6 comments on the relevance of the previous results for other pulsars, in particular for PSR 0656+14 and PSR 1055-52. Section 7 contains our conclusions.

2. GEMINGA

2.1. Geminga’s Age

The Geminga period as measured by Halpern & Holt (1992) is $P = 0.2370974 \text{ s} \pm 0.1 \mu\text{s}$. The earlier observation by *COS-B* and the later ones by *GRO* have slightly different P s which lie very accurately on a straight line (Bignami & Caraveo 1992) and give a practically constant period derivative of $\dot{P} = 1.099 \pm 0.001 \times 10^{-14} \text{ s s}^{-1}$ over a span of 16 yr. The corresponding spin-down age is $\tau = P/2\dot{P} = 3.4 \times 10^5 \text{ yr}$. This age is obtained with a braking index $n = 3$, i.e., with magnetic dipole braking. We will consider a range of ages corresponding to braking indices $n = 2$ and 4,

$$2.3 \times 10^5 \text{ yr} \leq t \leq 6.8 \times 10^5 \text{ yr}, \quad (1)$$

the upper value probably being an overestimate. We refer to Michel (1991) and Lyne & Graham-Smith (1990) for discussions of the reliability of the spin-down age as an indicator of the true age.

2.2. Geminga’s Temperature

In the first estimate of the star’s temperature, Halpern & Holt (1992) fitted the two apparent components of the spectrum with a blackbody and a power law. The best fit gave a blackbody temperature of $T = 3 - 4 \times 10^5$ K. In a second, more detailed analysis Halpern & Ruderman (1993) replaced the power-law component by a second blackbody with higher temperature and argued that this hotter component ($T \cong 3 \times 10^6$ K) is due to emission from a reheated polar cap (this temperature is too high to be explained only by the anisotropy of heat transport in the crust in presence of a magnetic field). They obtained for the main surface emission a temperature $T = 5.2 \pm 1.0 \times 10^5$ K. From the luminosities of these two components, they concluded that the ratio of the areas of the hot and cold emitting regions is about 3×10^{-5} . Moreover, it is likely that the surface is not emitting uniformly and that some colder region is not being seen, making the concept of “surface temperature” an ambiguous one. However, cooling calculations give as an output the effective temperature, i.e., a total luminosity, and the presence of a cooler region would reduce the luminosity and make the effective temperature somewhat lower than the inferred value of $5.2 \pm 1.0 \times 10^5$ K.

All these analyses use blackbody spectra, but the surface of a neutron star cannot be expected to be a perfect blackbody. Romani (1987) has calculated more realistic spectra for various surface chemical compositions without magnetic field. Miller (1992) and Shibano *et al.* (1992) have partially extended these results by including the magnetic field effects. The general trend of these results, for H or He atmospheres, is that there is an excess emission in the Wien tail of the spectrum, compared to a blackbody, and the excess falls within the *Einstein* and *ROSAT* detector ranges. This excess is reduced if metals are present (because of absorption edges) or when the effects of the magnetic field are taken into account. As a consequence, the use of these spectra would lower the measured temperature. Finally, some contamination from a surrounding nebula and/or some surface reheating by gamma rays or particles from the magnetosphere cannot be excluded. See Halpern & Ruderman (1993) for a discussion.

We will take for comparison with our calculations an effective temperature of

$$4 \times 10^5 \text{K} \leq T_e \leq 6 \times 10^5 \text{K} \tag{2}$$

but insist that it must be taken as an upper limit for the above mentioned reasons. Being determined from the spectrum, this temperature is independent of the distance, mass, and radius of the star and is the “temperature at infinity” T^∞ , i.e., the redshifted temperature.

3. THE PHYSICS OF NEUTRON STAR COOLING

At an age of a few multiples of 10^5 yr *Geminga* is well into the isothermal phase (Nomoto & Tsuruta 1987); its internal temperature T_i is uniform except for a gradient in the *envelope* just below the surface. The thermal evolution of the star is determined by energy conservation,

$$\frac{dE}{dt} = C_v \frac{dT_i}{dt} = -L_\nu - L_\gamma, \quad (3)$$

where E is the total thermal energy of the star, C_v its total specific heat, and L_ν and L_γ the total neutrino and photon luminosities (general relativistic correction factors are omitted here but were included in our calculations). The photon luminosity is $L_\gamma = 4\pi R^2 \sigma T_e^4 \propto T_i^{2.2}$, where the effective temperature T_e is converted into an internal temperature T_i according to the $T_i - T_e$ relationship calculated by Gudmundsson, Pethick & Epstein (1982, 1983). The neutrino emissivities are proportional to T_i^6 or T_i^8 (see Table 1), hence photon emission from the surface will eventually dominate over neutrino emission when the temperature has dropped sufficiently. This turnover happens before the star reaches 10^5 yr : *Geminga* is thus well into the *photon cooling era*. In this phase the cooling rate is mostly determined by the total specific heat of the star, but the actual surface temperature also depends on the previous neutrino cooling, which can be considered as giving the initial condition for photon cooling. Our cooling curves are calculated with the Heyney-type code already presented in Page & Baron (1990) and Page & Applegate (1992) which solves the general relativistic heat transport and energy balance equations. The reader is referred to these papers for more details.

3.1. Neutrino Processes

The dominant neutrino emission processes occur in the core of the star and are variants of beta and inverse beta decay. Table 1 shows the approximate emissivities of several processes for comparison. One can divide them into slow and fast neutrino emission, according to whether they involve four or two baryons. The large difference between slow and fast processes comes mainly from phasespace considerations: Fermi’s “Golden rule” tells us that the rate is proportional to the total phasespace volume available for both initial and final particles, and for fermions this volume is proportional to $k_B T / E_F$ where E_F is the particle Fermi energy. Typical nucleon Fermi energies in neutron star cores are of the order of a few tens to a few hundreds of MeV; if one takes a typical temperature

of $T = 10^9\text{K} \cong 0.1\text{MeV}/k_B$ and $E_F \sim 10^2 \text{ MeV}$ then a four fermion process is about $(k_B T/E_F)^2 \sim 10^{-6}$ time weaker than a two fermion process, which is what the direct Urca - modified Urca emissivities show (see Table 1). Participation of a meson (pion or kaon) in a process does not introduce any phase space limitation since these are bosons, but strong interactions effects, and strangeness violation in the case of kaons, reduce the efficiency of meson processes compared to the simple direct Urca process. Hyperons may also constitute a large fraction of the core baryons (see, e.g., Glendenning 1985) and will then participate into either modified (Maxwell 1987) or direct (Prakash et al. 1992) Urca processes, depending on their relative concentrations, but with somewhat lower emissivities compared to the corresponding nucleon processes. We refer to Pethick (1992) and Prakash (1993) for recent reviews of the neutrino emission problem. While there is still doubt about which fast process can actually occur, the number of presently proposed channels is so large that it is becoming difficult to believe that none of them is permitted and that neutron star cooling follows the old “standard” model with only the slow modified Urca process. Nevertheless, awaiting a conclusive argument on this point, we will still consider both the fast and slow cooling scenarios.

Deconfined quarks may be present in the center of massive neutron stars and are also copious neutrino emitters. They thus belong to the fast neutrino cooling scenario but obviously require a separate treatment. We will not consider them explicitly here.

3.2. The Boundary Condition

An important ingredient is the above mentioned $T_i - T_e$ relationship. Gudmundsson *et al.* (1982, 1983) were the first to present a detailed study of it but did not include the effect of the magnetic field \vec{H} which enhances the heat transport parallel to \vec{H} and strongly suppresses it in the perpendicular direction. The extensive magnetic envelope calculations of Hernquist (1985) and Van Riper (1988) for transport parallel to \vec{H} show that for a given inner temperature T_i the surface temperature T_s is raised, compared to the nonmagnetic case, but by no more than 50% even with a field of 10^{14} G (the surface magnetic field of Geminga is estimated to be about 1.6×10^{12} G). When the field is at an angle to the surface, T_s should be lower, and by simple geometric considerations Hernquist (1985) argued that the magnetic effects when including a global field configuration are probably very small. Schaaf (1990a,b) has performed envelope calculations with an arbitrary orientation of \vec{H} with respect to the surface, and his results can be used to estimate the surface temperature distributions $T_s(\theta, \phi)$ resulting from various magnetic field configurations

and the corresponding effective temperatures T_e . Preliminary results (Page 1994) confirm Hernquist's point that the $T_i - T_e$ relationship depends only weakly on the magnetic field. We will consequently use the zero-field relationship here, which should introduce an error of no more than a few percent.

3.3. The High-Density Equation of State

The equation of state (EOS) has two functions in our models, the first being simply to give the global structure of the star, i.e., the density versus radius profile as a solution of the Oppenheimer-Volkoff equation of hydrostatic equilibrium, and the second being to determine the chemical composition. Obviously, the slow and fast neutrino cooling cases are associated with quite different EOSs at supranuclear density, and we will discuss them separately.

For modeling the slow neutrino cooling, we consider five different EOSs from modern calculations: one relativistic, MPA (Müther, Prakash & Ainsworth 1987), two nonrelativistic, FP (Friedman & Pandharipande 1981) and WFF(av14) (Wiringa, Fiks & Fabrocini 1988), and two parametric, PAL32 and PAL33 (together PAL: Prakash, Ainsworth & Lattimer 1988), whose properties are intermediate to the above three. Each one of these calculations gives the energy per baryon for neutron matter and symmetric nuclear matter, from which we obtain the EOS for matter in β -equilibrium and the chemical composition following Wiringa *et al.* (1988), or Prakash *et al.* (1988) for PAL. The properties of these EOSs related to neutron stars are summarized in Table 2; they encompass a broad range of stiffness with maximum masses of $1.68 M_{\odot}$ - $2.44 M_{\odot}$, proton fractions in a $1.4 M_{\odot}$ star of 2.0% - 11.4% and radii of a $1.4 M_{\odot}$ star of 10.6 km - 12.5 km. We have rejected EOSs with proton fractions large enough to allow the direct Urca process in a $1.4 M_{\odot}$ star, but do consider MPA, PAL32, and PAL33 which allow it at higher masses (notice that the PAL32 EOS gives a $1.4 M_{\odot}$ star on the verge of allowing the direct Urca process). Two EOSs, BPS (as listed in Baym, Pethick & Sutherland 1971) and PS (Pandharipande, Pines & Smith 1976) have been very popular in neutron star cooling studies. We do not use the BPS EOS for modeling the slow cooling since this extremely soft EOS (which gives a density above 10 times nuclear matter density in the center of a $1.4 M_{\odot}$ star) is actually built on a high-density EOS with hyperons (Pandharipande 1971) in which the hyperonic direct Urca is allowed and this EOS thus belongs to the fast neutrino cooling case (hyperons appear at a star mass of $0.4 M_{\odot}$ in this model). The softening of this EOS is due in an essential way to the presence of the hyperons, and nothing similar can be expected with only nucleons. The PS EOS has already been considered in previous works (Nomoto & Tsuruta 1986, 1987; Van Riper 1991), and we will simply quote their results below. However, in this extremely stiff EOS the neutrons form a three-dimensional lattice and thus have a totally different specific heat and a different neutrino emissivity than liquid neutrons, two facts not taken into account in the models, and the stiffness of this EOS is inseparable from to the lattice structure.

The choice of the EOS for fast neutrino cooling models is not as important as for slow

cooling at the present stage of development of the theory. There are several other factors which have much more influence, for example the critical density at which fast neutrino emission turns on, the fast neutrino emission which is actually at work, the occurrence of baryon pairing, etc., all of which are at best poorly known. Therefore, calculations of fast cooling have often been done with various EOSs in a partially justified, careless way. However, one model has been developed with much detail, based on the ALS model of dense matter (Takatsuka *et al.* 1978), which is somewhat inspired by the PS EOS, but where the lattice structure is one-dimensional and where two-dimensional nucleon pairing occurs in planes orthogonal to the lattice direction (see Tamagaki 1992 for a general description). In this model, charged pion condensation develops at high density, but the resulting EOS is close to the FP EOS at low density below the condensation threshold, i.e., the stiffness of the PS EOS has disappeared. Cooling calculations within the ALS model have been performed by Umeda *et al.* (1992), and their results will be used below.

3.4. Nucleon Pairing

Pairing *à la* BCS (superfluidity) of the nucleons in the neutron star core has a dramatic effect on the cooling because it suppresses both the neutrino emission and the specific heat. The pairing is in the 1S_0 partial wave at low density and then shifts to the 3P_2 partial wave at higher density. The protons in the core and the neutrons in the inner crust are expected to be paired in the 1S_0 partial wave while the neutron pairing shifts to the 3P_2 partial wave in the core. The pairing of protons in the 3P_2 partial wave seems never to have been considered, probably on the grounds that its critical temperature would be very low. At still higher densities, the pairing should shift to the 1D_2 partial wave (the next partial wave in which the free nucleon-nucleon interaction is attractive), but the estimated corresponding critical temperature is too low for this type of pairing to be of any interest (Amundsen & Østgaard 1985b). Theoretical calculations of T_c are extremely difficult and the presently published values are still highly uncertain except in the case of crust neutron 1S_0 pairing, where reasonable agreement has been obtained between the various latest calculations. Figure 1 shows most of the presently published calculations of critical temperatures for core neutron and proton pairings. One sees that both the maximum value of T_c and the density range where it is nonzero are very uncertain, particularly in the neutron case. For the 1S_0 proton pairing, the latest calculation (Wambach, Ainsworth & Pines 1991) was the first to include in a consistent way the neutron background and shows a strong *reduction* of T_c , but with a density dependence apparently different from that found in earlier calculations. However, this result depends strongly on the relative densities of neutrons and protons,

and thus, calculations with a different proton fraction (a poorly known quantity) may give quite different results (Ainsworth 1992). Medium dispersion effects (i.e., change in the nucleon effective mass) have an enormous effect, as shown in Figure 1b by the differences between the curves AO and T72, where the effective mass $m^* \equiv M^*/M$ is obtained in a self-consistent way and the corresponding curves labeled with $m^* = 1$ for which the effective mass is forced to the free mass value. (The Hoffberg *et al.* 1970 calculation used $m^* = 1$.) Of course, m^* is also poorly known at high density. Further extensive calculations within the ALS model (Takatsuka & Tamagaki 1982, and references therein) with and without pion condensation give values of T_c for 3P_2 neutron pairing that are between the two extremes shown in Figure 1b as T72 and T72($m^* = 1$). For 3P_2 neutron pairing, background effects beyond the first order ones considered in the results shown in Figure 1b and similar to the effects considered by Wambach *et al.* (1991) for 1S_0 proton pairing have been studied (Jackson *et al.* 1982). The results indicate that, in this case, background effects strongly *enhance* the pairing; thus, values of T_c higher than shown in Figure 1b and extending to higher densities are quite possible. In light of this, the case for proton 3P_2 pairing should also be considered seriously, as should 1D_2 pairing. In other words, we know neither the value of T_c in the core nor the relevant density range, neither for neutrons nor for protons, but it is reasonable to expect large values extending to high densities. If hyperons are present, one can expect that they will also pair for the same reasons nucleons do. With regard to quarks, pairing is also very probable (Bailin & Love 1984).

The effect of pairing is to reduce the phase space available for excitations. As a result, both the specific heat of the paired component and the neutrino processes in which it participates will be suppressed. We treat this effect on C_v following Levenfish & Yakovlev (1993; see also Gnedin & Yakovlev 1993), who performed detailed calculations of the reduction factors in cases both of isotropic 1S_0 and anisotropic 3P_2 pairing. For the neutrino emissivity suppression, we simply use a Boltzmann factor $\exp(-\Delta/kT)$, where Δ is the pairing gap, which is not very accurate but has no serious consequence here since we consider only the photon cooling era.

4. FAST NEUTRINO COOLING SCENARIOS

Fast neutrino cooling encompasses a variety of different scenarios, kaon or pion condensate, direct Urca with nucleons and/or hyperons and/or isobars, quark matter, and so forth which share the characteristic that their neutrino emissivities are many orders of magnitude higher than the modified Urca process emissivity. As a result, whenever one of

these processes is allowed to operate freely, the resulting surface temperature, once the star has reached isothermality, is far below any of the presently available observational estimates (Page & Baron 1990; Van Riper 1991; Page & Applegate 1992; Page 1992; Umeda *et al.* 1992), including the new Geminga observation. This raw picture is strongly altered if the neutrino-emitting baryons (nucleons, hyperons, quarks, etc.) become paired. As presented by Page (1989) for the kaon condensate case and by Page & Applegate (1992) for the direct Urca with nucleons case, the early suppression of the neutrino emission due to the pairing gap can keep the surface temperature T_s , after isothermalization and until an age of about 10^5 yr, anywhere between approximately 2×10^5 K and 1.5×10^6 K. The actual value of T_s is then only a function of the pairing critical temperature T_c of the neutrino emitting fluid(s) (to be precise, since T_c is density dependent, T_s is a function of the lowest value of T_c within the “pit” of fast neutrino emission). In a multicomponent system like nucleons + hyperons, various direct Urca processes can operate simultaneously (Prakash *et al.* 1992), and, for the star not to drop into invisibility, all of them have to be stopped by having one of the participating baryons paired. In particular, if both Λ and Σ^- are present together, they undergo a purely hyperonic direct Urca process, and thus, one of them must be paired. One can expect that T_c is lower for hyperons than for nucleons if the former have weaker interactions than the latter, and the star’s temperature would then be controlled by hyperon pairing.

The models of Page & Baron (1990), Umeda *et al.* (1992), and Page & Applegate (1992) of kaon, pion, and nucleon direct Urca cooling, respectively, with superfluidity suppression easily accommodate the estimated surface temperature of Geminga. The crucial point, however, is that pairing has to occur down to the very center of the star and the critical temperature must be higher than 10^9 K everywhere. If even a very small region is left unpaired, it will drive the surface temperature well below the observed value of 5×10^5 K. For example, the $1.4 M_\odot$ case of Page & Applegate (1992), with a direct Urca emitting pit of only $0.038 M_\odot$, has a temperature of 1.5×10^5 K at Geminga’s age if pairing does not occur. Such a low surface temperature would make Geminga’s surface practically unobservable by *ROSAT* (the hot polar cap would of course still be seen).

It is not possible to distinguish between the various neutrino emission processes from this analysis only: both a kaon (or pion) condensate and the direct Urca, even if their emissivities differ by three orders of magnitude, are compatible with the Geminga data when pairing is taken into account, but with different values for T_c . The T_c values needed are within the range of theoretical predictions, but this range is so large it can accommodate almost any data. Moreover, even within one given neutrino emission scheme very different values of T_c are possible: for example the models labeled HGRR and 0.1HGRR of Fig. 2 in Page & Applegate (1992), i.e., direct URCA and 3P_2 neutron pairing with T_c from

Hoffberg *et al* (1970) or with the same T_c multiplied by 0.1, are both acceptable within the observational uncertainty in the Geminga data.

It should be mentioned that internal heating by friction of the crust neutron superfluid can significantly alter the thermal evolution of a neutron star when its temperature, and thus its specific heat, is low. The models of fast cooling with pions and heating of Umeda *et al.* (1993), without core nucleon pairing, can produce a star with a surface temperature at Geminga’s age of at most 3×10^5 K *when heating is at its maximum strength* (instead of 1.5×10^5 K without heating). This is lower than the Geminga temperature considered here (measured with a blackbody spectrum) but may be high enough if Geminga is actually cooler.

5. THE SLOW NEUTRINO COOLING SCENARIO

Slow neutrino cooling is a well-defined scenario based on the conservative hypothesis that the neutron star core is made exclusively of neutrons and protons (plus electrons and muons to preserve charge neutrality, but no charged pions, kaons, quarks, etc.) with a proton fraction low enough for the direct Urca process to be forbidden (Lattimer *et al.* 1991), and its predictions for surface temperatures are much more restrictive than those of the fast neutrino cooling scenarios. We defer a detailed study to later work and only analyze here the photon cooling era relevant to Geminga.

The photon energy loss can be calculated accurately since the core temperature-effective temperature relationship is known quite accurately, even in presence of a magnetic field. We take the core neutrino emissivity of the modified Urca process and the two associated neutral current bremsstrahlung processes from Friman & Maxwell (1979). Of critical importance here is the total specific heat of the star, which depends on the EOS and chemical composition (proton fraction). Pairing of nucleons is essential here because of its suppression of the specific heat. Table 3 shows the contribution to the normal (i.e., without pairing) specific heat of the various components in a $1.4 M_\odot$ star at a temperature $T = 10^9 K$ for our five EOSs. Pairing will suppress C_v exponentially when $T \ll T_c$ and the corresponding specific heat will practically disappear. In all our calculations, the crust neutrons are paired using the gap from Ainsworth, Wambach & Pines (1989) and their contribution to C_v is thus strongly reduced; the crust electrons make a negligible contribution as does the crust lattice. One can see from Table 3 that the core neutrons contribute about three-fourths of the total specific heat, the protons one-fourth and the core electrons about 5%, independent of the EOS.

Because of the large theoretical uncertainty about the actual value of the pairing critical temperature T_c for both neutrons and protons in the core as well as the uncertainty on the density dependence of T_c we first consider density independent T_c ; i.e., we force pairing in the whole core and take $T_c = 2 \times 10^9$ K. The resulting cooling curves of a $1.4 M_\odot$ star for our five EOSs are shown in Figures 2a-2d and are compared with the Geminga data. Because in this photon cooling era the determining factor is the total specific heat, the five EOSs give basically identical results since the contribution of the various components to C_v is only weakly dependent on the EOS and pairing, when assumed, is present in the whole core. When none of the core nucleons is paired (a) the theoretical results are consistent only with the higher surface temperature T_s and the older age: considering that this T_s is certainly an overestimate, one can state that Geminga’s temperature is incompatible with these cooling models (unless Geminga’s age is underestimated, but spin-down ages are usually considered to be overestimates). With pairing of the protons (b) the discrepancy increases because the small ($\sim 25\%$) decrease of the specific heat in the photon cooling era is not sufficient to compensate for the significant reduction of the earlier core neutrino emission (during which only the very slow nn bremsstrahlung is unaffected), which gives a high temperature at the beginning of the photon cooling era. When all the core neutrons are paired (c) the reduction of C_v is large enough to accomodate the observed temperature. If both neutrons and protons are paired within the whole core (d) C_v is cut by a factor of 20 (only the electron and muon contributions are left) and the temperature drop during the photon cooling era is extremely fast; however, heating mechanisms (Shibazaki & Lamb 1989; Cheng et al. 1992; Umeda *et al.* 1993) could slow the cooling and keep the temperature compatible with Geminga. These results were at a fixed mass of $1.4 M_\odot$, but Figure 3 shows that changing the star mass makes little difference as long as pairing is still assumed throughout the whole core. With realistic density dependent gaps, by varying the star’s mass we change the fraction of core baryons paired, and any temperature between the extreme cases of Figures 2b and 2d could in principle be obtained.

Figure 4 shows three cooling curves with three published calculations of 3P_2 neutron pairing and the EOS WFF(av14) for a $1.4 M_\odot$ star. (The Fermi momentum of the neutrons in the center of the star, for comparison with Fig. 1, is $k_F(n) = 2.58 fm^{-1}$). The pairing of Takatsuka (1972) has almost no effect, since T_c vanishes at low density and most of the core is left unpaired. The two calculations of Hoffberg *et al.* (1970) and Amundsen & Østgaard (1985b) give almost identical results in the photon cooling era, since in both cases the whole core is paired and the internal temperature T_i is much lower than T_c ; in both cases, the whole core neutron specific heat has been practically eliminated. In the neutrino cooling era where T_i is higher these two cases do differ significantly (their T_c differ by an order of magnitude): in the Hoffberg *et al.* (1970) case, the core neutrino emission is

practically turned off early on due to the very high T_c , while in the Amundsen & Østgaard (1985b) case, the suppression happens much later and is thus less efficient. It is thus not possible to deduce any value for T_c from the Geminga data only, except that it must be higher than a few multiples of 10^8 K, but we can state that pairing must occur within most of the core. Published cooling curves with the PS EOS (Nomoto & Tsuruta 1986, 1987; Van Riper 1991) also fit the Geminga data, in their superfluid versions where the neutrons are paired in the whole core.

6. COMMENTS

6.1. The Cooling of Low-Mass Neutron Stars

The surface temperatures we have obtained with the slow neutrino cooling scenario during the photon cooling era when both neutrons and protons are paired within the whole core (Fig. 2d) are much lower than any prediction previously published. This is so because 95% of the star’s specific heat has been suppressed by superfluidity when all core nucleons are paired. This case has to be seriously considered for low-mass neutron stars, where there is little doubt that pairing happens down to the center of the star for both neutrons and protons, and it has some unexpected effects. Consider, e.g. as shown in Figure 5, the case of a heavy star undergoing fast neutrino cooling with suppression from neutron 3P_2 pairing but with a core that still has a substantial amount of unpaired protons. If the critical temperature for neutron pairing is a few multiples of 10^9 K, during the neutrino cooling era the star will have a lower temperature than a slow neutrino cooling star of low mass, but later during the photon cooling era it will be much warmer than the lighter (wholly paired) star. Thus *fast neutrino cooling does not mean fast cooling forever*.

If one adopts the idea that the critical density for the onset of fast neutrino emission is low, then it is quite possible that all neutron stars undergoing slow neutrino cooling, and thus having very low central densities, have both their neutrons and their protons paired within the whole core with high values of T_c . All neutron stars undergoing slow neutrino cooling would then cool very quickly in the photon cooling era and would become invisible after a couple of hundreds of thousands of years. Consequently, any neutron star older than that, with detectable surface thermal emission, has an unpaired baryonic core component, which provides the star with a sizable specific heat, but has undergone fast neutrino emission suppressed early on by pairing of its other core component(s).

6.2. “Standard” Cooling ?

However, there may not even be such a thing as a slow neutrino cooling (“standard” cooling) neutron star since, as mentioned in the introduction, the number of presently proposed channels for fast neutrino emission is so large, and the corresponding critical densities so low in some cases, that it is possible that *all* neutron stars cool by some fast neutrino process. If this is the case, the thermal evolution of all neutron stars is entirely controlled by superfluidity. The surface temperature from age $\sim 10^2$ yr to $\sim 10^5$ yr depends on the minimal value of T_c for the relevant neutrino emitting baryonic component (nucleon or hyperon) in the core (Page & Applegate 1992), and the temperature from age $\sim 10^5$ yr to $\sim 10^6$ yr depends on how much of the core is left unpaired. It is worth mentioning here that observational support for the “standard” model is actually extremely dim, if not nonexistent. It has traditionally been based (Tsuruta 1986) on *Einstein* observations of the Crab pulsar (Harnden & Seward 1984) and of the two compact objects detected in the supernova remnants 3C58 (Becker *et al.* 1982) and RCW 103 (Tuohy *et al.* 1983), all three having ages ~ 1000 yr and upper limits on temperature of the order of $2 - 3 \times 10^6$ K. However, none of these three temperature estimates can be given much credibility for the following reasons: 1) *ROSAT* has failed to detect the previously seen source in RCW 103 (Becker *et al.* 1993); no matter what this object is, or was, it is not a neutron star cooling according to the slow neutrino emission scenario. 2) The temperature estimate for the 3C58 central source was based on an assumed distance of 8 kpc which was later reduced by a factor of 3 (Green & Gull 1982): with this new distance, the resulting temperature would be low enough to be marginally inconsistent with the “standard” cooling model. Moreover the age of 3C58 is based on an association with the A.D. 1191 supernova, but Becker *et al.* (1982) questioned this association, arguing from the low ratio of X-ray to radio luminosities of the remnant that it is probably much older; this would ruin its relevance for comparison with models of early cooling of neutron stars. 3) For the Crab pulsar (the only case of these three whose existence and age are beyond doubt), the temperature estimate is based on an upper limit of the flux between the pulses of the X-ray curve observed by *Einstein*: the pulsar is *undetected* at this phase, and thus the temperature can hence be anywhere below the reported upper limit of 2.5×10^6 K. In none of these three cases was there any spectral evidence that the X-ray emission is thermal emission from the surface of the star, since the Crab and RCW 103 observations were done with the HRI detector, which had no energy resolution, and the count rate from the 3C58 point source in the IPC detector was too low to provide useful spectral information. Moreover, the magnetospheric X-ray emission from such young neutron stars is so strong that there is little hope of detecting thermal radiation from the surface of the star itself (Ögelman 1993). A fourth neutron star young enough to allow us to distinguish between slow and fast neutrino cooling, and in this case

with good data, is PSR 0833-45 (Vela): comparisons with theoretical models have shown repeatedly that its surface temperature is too low for “standard” cooling and requires a fast cooling agent (Nomoto & Tsuruta 1986; Shibazaki & Lamb 1989; Page & Baron 1990; Van Riper 1991; Page & Applegate 1992; Umeda *et al* 1992, 1993). It is therefore a reasonable theoretical *a priori* to interpret all data within the fast neutrino cooling scenario. Nevertheless, as stated in section 3.1, we still consider both types of neutrino cooling, letting observation be the ultimate judge.

6.3. PSR 0656+14 and PSR 1055-52

Since analyses of the *ROSAT* observations of PSR 0656+14 and PSR 1055-52 have been published recently, we will now briefly comment on these results in light of the preceding remarks. The data are plotted in Figure 6, along with some typical cooling curves.

In the case of PSR 0656+14, when the spectral fit is done with a blackbody, the resulting surface temperature is $9.0 \pm 0.4 \times 10^5$ K, while a nonmagnetic helium atmosphere gives $2.2 \pm 0.2 \times 10^5$ K (Finley *et al.* 1992). For a spin-down age of 1.1×10^5 yr the first value is perfectly compatible with the slow neutrino cooling scenario (without core pairing or with an appropriate proportion of core baryons paired), while the second is in disagreement and needs fast neutrino cooling, unless the star is older than its spin-down age. An analysis with a magnetic hydrogen atmosphere spectrum gives an intermediate value of $6.9_{-0.3}^{+0.5} \times 10^5$ K (Anderson *et al.* 1993), which is lower than previously predicted for slow neutrino cooling but slightly higher than our new results in the case of complete pairing of the core: this temperature can easily be accommodated within this model by having almost complete pairing of neutrons and protons in the core, i.e. by slightly increasing the total specific heat compared to the completely paired case. PSR 0656+14 would have to be much younger than its spin-down age indicates for the magnetic temperature estimate to be incompatible with the slow neutrino cooling scenario.

For PSR 1055-52, spectral fits with a blackbody give a surface temperature of $7.0 \pm 0.6 \times 10^5$ K (Ögelman & Finley 1993). Given the spin-down age of 5×10^5 years, Ögelman & Finley conclude that this temperature is compatible with the slow neutrino cooling models: this is true only for models *without pairing in the core* or with only protons paired. This temperature is slightly too high compared to slow cooling with neutron core pairing, but heating may explain the discrepancy, and moreover, fits with non black-body spectra will give lower temperatures and require less heating, if any at all. If both neutrons and protons are paired within the whole core, the theoretical temperature with slow

neutrino cooling is much lower than the 7×10^5 K reported. If we compare this result with those from the heating models of Shibazaki & Lamb (1989) and Cheng *et al* (1992) only the maximum heating rates of these models could justify the discrepancy in this case: thus, *PSR 1055-52 most probably contains an unpaired component in its core*. Being more speculative, if one adopts the idea that the critical density for fast neutrino emission is low and that, consequently, all neutron stars undergoing slow neutrino cooling have their whole core paired and follow the trajectory of Figure 2d, then this reported temperature of 7×10^5 K is incompatible with the slow neutrino cooling scenario unless a very efficient heating mechanism is at work.

7. CONCLUSIONS

We have compared the recent temperature measurement of the Geminga neutron star with cooling models and found that, since this star is old enough to be in the photon cooling era, both fast and slow neutrino emission mechanisms can explain its temperature. One therefore cannot draw any conclusion about neutrino emission from dense nuclear matter using this observation alone. However, *a crucial feature in both types of models is that they need nucleon pairing in most, if not all, of the core*. If no pairing is assumed in the core, then the predicted temperature is either too high (slow neutrino cooling) or too low (fast neutrino cooling) when compared to the observed temperature of Geminga.

With fast neutrino cooling, nucleon pairing is needed to stop the early cooling which, without this, would produce a star with a temperature much lower than what is observed. If the fast neutrino emission is from hyperonic processes it is possible that the suppression we observe is due to hyperon superfluidity. It is not possible to distinguish between the various fast processes, however; the theoretical uncertainty about T_c allows us to accommodate very different neutrino emission rates. Moreover, within a given fast cooling scenario, the observational uncertainty also allows very different values of T_c . However, since fast neutrino emission occurs down to the very center of the core, to be compatible with the Geminga observation, these scenarios need pairing up to the highest density reached in this object, with pairing critical temperatures higher than 10^9 K.

Within the slow neutrino cooling model (the “standard” model), superfluidity is also needed, but for a different reason. The observed temperature is below what the simple model without pairing predicts, but since this star is cooling by photon emission, we can accelerate the cooling at this time by decreasing the specific heat through pairing. The theoretical curves, in the photon cooling era, are very insensitive to the high-density EOS

or the star mass, the only determining factor being how much of the core specific heat has been eliminated by pairing. If we accept an age of 3×10^5 yr and a temperature of 5×10^5 K, then the specific heat must have been reduced to about 25% of its normal value. This can be obtained either by pairing of the neutrons in the whole core or by a combination of neutron and proton pairing, but even in this case most of the neutrons must be paired. If both neutrons and protons are paired in the whole core, photon cooling becomes so efficient that a substantial amount of heating is needed, but several possible mechanisms have been proposed and may be able to provide sufficient heating.

The above discussion shows that, in order to distinguish clearly between the fast and slow neutrino cooling scenarios, we need observations of neutron stars younger than 5×10^4 yr, for which the slow cooling scenario predicts temperatures higher than $0.9 - 1.1 \times 10^6$ K, depending on the exact age; at later times, both scenarios can accommodate most observable temperatures depending on the amount of pairing assumed. Geminga is old enough that the effect of the early neutrino cooling has been washed out. However, our analysis showed that this star does tell us -independently of its earlier neutrino cooling history- that most, if not all, of its core is paired. PSR 0656+14 is at the limit at which we can still distinguish the effect of fast neutrino cooling, but the present uncertainty about its temperature precludes drawing any conclusion. PSR 1055-52 can be also interpreted within both types of neutrino scenarios, but its core must contain an unpaired component whose specific heat keeps the star warm despite its age. If one accepts the fast neutrino cooling scenario as universal (a reasonable theoretical *a priori*), then these three objects show evidence of baryon pairing down to their very center, needed for suppression of early neutrino emission, but none of them requires this scenario.

I am grateful to T. Ainsworth, J. H. Applegate, J. P. Halpern, M. Prakash, and M. Ruderman for discussions. This work was supported by HEA-NASA grant NAGW 3075 and, in its early phases, by a fellowship from the Swiss National Science Foundation. This work is contribution number 544 of the Columbia Astrophysics Laboratory.

Process Name	Process	Emissivity Q_ν (erg/sec/cm ³)
a) Modified URCA	$\begin{cases} n + n' \rightarrow n' + p + e^- + \bar{\nu}_e \\ n' + p + e^- \rightarrow n' + n + \nu_e \end{cases}$	$\sim 10^{20} \cdot T_9^8$
b) K-condensate	$\begin{cases} n + K^- \rightarrow n + e^- + \bar{\nu}_e \\ n + e^- \rightarrow n + K^- + \nu_e \end{cases}$	$\sim 10^{24} \cdot T_9^6$
c) π^- - condensate	$\begin{cases} n + \pi^- \rightarrow n + e^- + \bar{\nu}_e \\ n + e^- \rightarrow n + \pi^- + \nu_e \end{cases}$	$\sim 10^{26} \cdot T_9^6$
d) Direct URCA	$\begin{cases} n \rightarrow p + e^- + \bar{\nu}_e \\ p + e^- \rightarrow n + \nu_e \end{cases}$	$\sim 10^{27} \cdot T_9^6$
e) Quark URCA	$\begin{cases} d \rightarrow u + e^- + \bar{\nu}_e \\ u + e^- \rightarrow d + \nu_e \end{cases}$	$\sim 10^{26} \alpha_c T_9^6$

Table 1: Some core neutrino emission processes and their emissivities. The emissivities are from : a) Friman & Maxwell 1979, b) Brown *et al* 1988, c) Maxwell *et al* 1977, d) Lattimer *et al* 1991 and e) Iwamoto 1980. T_9 is the temperature in units of 10^9 kelvins.

EOS	Maximum-Mass Star			1.4 M_{\odot} Star		
	$M(M_{\odot})$	$\rho_c(fm^{-3})$	$x_p(\%)$	$R(km)$	$\rho_c(fm^{-3})$	$x_p(\%)$
FP	1.79	1.18	~ 0	10.85	0.69	2.0
WFF(av14)	2.10	1.25	4.8	10.60	0.64	9.6
MPA	2.44	0.89	19.0	12.45	0.41	9.0
PAL32	1.68	1.51	15.2	11.02	0.74	11.4
PAL33	1.90	1.24	14.0	11.91	0.54	9.7

Table 2: Some properties of the EOS’s used for slow neutrino cooling. Columns two to four list the mass, central density and central proton fraction of a maximum mass star. Columns five to seven give properties of a 1.4 M_{\odot} star : radius, central density and central proton fraction. (The PAL EOSs are labeled PALij, i,j=1,2,3, where i refers to the symmetry energy function and j to the compression modulus)

EOS	Core Components			Crust Components	
	n	p	e	n	e
FP	9.89	2.89	0.50	0.97	0.025
WFF(av14)	9.31	2.81	0.51	0.72	0.018
MPA	11.90	3.90	0.67	1.60	0.044
PAL32	9.66	3.41	0.68	1.16	0.031
PAL33	10.96	3.72	0.68	1.42	0.037

Table 3: Normal specific heat, at $T = 10^9$ K, of neutrons, protons and electrons in the core and crust of a $1.4 M_{\odot}$ neutron star built with the five EOS's used for slow neutrino cooling. (Units are $10^{38} \text{ ergs } K^{-1}$, i.e. $C_v(T) = (\text{Table} - \text{Entry}) \times (T/10^9 K) \times 10^{38} \text{ ergs } K^{-1}$).

REFERENCES

- Ainsworth, T. L. 1992, private communication
- Ainsworth, T. L., Wambach, J. & Pines, D. 1989, *Phys. Lett.*, B222, 173
- Amundsen, L. & Østgaard, E. 1985a, *Nucl. Phys.*, A437, 487
- Amundsen, L. & Østgaard, E. 1985b, *Nucl. Phys.*, A442, 163
- Anderson, S. B., Córdova, F. A., Pavlov, G. G., Robinson, C. R. & Thompson, Jr, R. J. 1993, *ApJ*, 414, 867
- Bailin, D. & Love, A. 1984, *Phys. Rep.*, 107, 325
- Baym, G., Pethick, C. J. & Sutherland, P. 1971, *ApJ*, 170,299
- Becker, R. H., Helfand, D. J. & Szymkowiak, A. E. 1982, *ApJ*, 255, 557
- Becker, W., Trümper, J., Hasinger, G. & Aschenbach B. 1993, in *Isolated Pulsars*, ed. K. A. Van Riper, R. Epstein & C. Ho (Cambridge: Cambridge Univ. Press) 116
- Bignami, G. F. & Caraveo, P. A. 1992, *Nature*, 357, 287
- Brown, G. E., Kubodera, K., Page, D. & Pizzochero, P. 1988, *Phys. Rev.*, D37, 2042
- Chao, N.-C., Clark, J. W. & Yang, C.-H. 1972, *Nucl. Phys.*, A179, 320
- Cheng, K. S., Chau, W. Y., Zhang, J. L. & Chau, H. F. 1992, *ApJ*, 396, 135
- Finley, J. P., Ögelman, H. & Kiziloğlu, Ü 1992, *ApJ*, 394, L21
- Friedman, B. & Pandharipande, V. R. 1981, *Nucl. Phys.*, A361, 502
- Friman, B. L. & Maxwell, O. V. 1979, *ApJ*, 232, 541
- Gehrels, N. & Chen, W. 1993, *Nature*, 361, 706
- Glendenning, N. K. 1985, *ApJ*, 293, 470
- Gnedin, O. Y. & Yakovlev, D. G. 1993, *Astron. Lett.*, 19, 104
- Green, D. A. & Gull, S. F. 1982, *Nature*, 299, 606
- Gudmundsson, E. H., Pethick, C. J. & Epstein, R. I. 1982, *ApJ*, 259, L19
- Gudmundsson, E. H., Pethick, C. J. & Epstein, R. I. 1983, *ApJ*, 272, 286
- Halpern, J. P. and Holt, S. S. 1992, *Nature*, 357, 222
- Halpern, J. P. & Ruderman, M. 1993, *ApJ*, 415, 286
- Harnden, F. R. & Seward, F. D. 1984, *ApJ*, 283, 279
- Hernquist, L. 1985, *MNRAS*, 213, 313

- Hoffberg, M., Glassgold, A. E., Richardson, R. W. & Ruderman, M. 1970, *Phys. Rev. Lett.*, 24, 775
- Iwamoto, N. 1980, *Phys. Rev. Lett.*, 44, 1637
- Jackson, A. D., Krotscheck, E., Meltzer, D. E. & Smith, R. A. 1982, *Nucl. Phys.*, A386, 125
- Lattimer, J. M., Pethick, C. J., Prakash, M. & Haensel, P. 1991, *Phys. Rev. Lett.*, 66, 2701
- Levenfish, K. P. & Yakovlev, D. G. 1993, in *Strongly Coupled Plasma Physics*, ed. H. M. Van Horn & S. Ichimaru (Rochester: University of Rochester Press)
- Lyne, A. G. & Graham-Smith, F. 1990, *Pulsar Astronomy*, (Cambridge: Cambridge University Press)
- Maxwell, O. V. 1987, *ApJ*, 316, 691
- Maxwell, O. V., Brown, G. E., Campbell, D. K., Dashen, R. F. & Manassah, J. T. 1977, *ApJ*, 216, 77
- Michel, F. C. 1991, *Theory of Neutron Star Magnetospheres*, (Chicago: Univ. Chicago Press)
- Miller, M. C. 1992, *MNRAS*, 255, 129
- Müther, H., Prakash, M. & Ainsworth, T. L. 1987, *Phys. Lett.*, B199, 469
- Niskanen, J. A. & Sauls, J. A. 1981, preprint
- Nomoto, K. & Tsuruta, S. 1986, *ApJ*, 305, L19
- Nomoto, K. & Tsuruta, S. 1987, *ApJ*, 312, 711
- Ögelman, H., 1991, in *Neutron Stars: Theory and Observation*, ed. J. Ventura & D. Pines (Dordrecht: Kluwer Academic Publisher) 87
- Ögelman, H., 1993, in *Isolated Pulsars*, ed. K. A. Van Riper, R. Epstein & C. Ho (Cambridge : Cambridge University Press) 96
- Ögelman H. & Finley J. P. 1993, *ApJ*, 413, L31
- Page, D. 1989, Ph.D. thesis, SUNY Stony Brook
- Page, D. 1992, in *Proc. 1st Symp. Nuclear Physics in the Universe*, ed. M. R. Strayer & M. W. Guidry (Bristol: Adam Hilger) 151
- Page, D. 1994, in preparation
- Page, D. & Applegate, J. H. 1992, *ApJ*, 394, L17
- Page, D. & Baron, E. 1990, *ApJ*, 354, L17; Erratum in *ApJ*, 382, L111
- Pandharipande, V. R. 1971, *Nucl. Phys.*, A178, 123

- Pandharipande, V. R., Pines, D. & Smith, R. A. 1976, *ApJ*, 208, 550
- Pethick, C. J. 1992, *Rev. Mod. Phys.*, 64, 1133
- Prakash, M. 1993, *Phys. Rep.*, in press
- Prakash, M., Ainsworth, T. L. & Lattimer, J. M. 1988, *Phys. Rev. Lett.*, 61, 2518
- Prakash, M., Prakash, M., Lattimer, J. & Pethick, C. J. 1992, *ApJ*, 390, L77
- Romani, R. W. 1987, *ApJ*, 313, 718
- Schaaf, M. E. 1990a, *A&A*, 227, 61
- Schaaf, M. E. 1990b, *A&A*, 235, 499
- Shibanov, Y. A., Zavlin, V. E., Pavlov, G. G. & Ventura, J. 1992, *A&A*, 266, 313
- Shibazaki, N. & Lamb, F. K. 1989, *ApJ*, 346, 808
- Takatsuka, T. 1972, *Prog. Theor. Phys.*, 48, 1517
- Takatsuka, T. 1973, *Prog. Theor. Phys.*, 50, 1754
- Takatsuka, T. & Tamagaki, R. 1982, *Prog. Theor. Phys.*, 67, 1649
- Takatsuka, T., Tamiya, K., Tatsumi, T. & Tamagaki, R. 1978, *Prog. Theor. Phys.*, 59, 1933
- Tamagaki, R. 1992, *Physica*, B178, 13
- Tsuruta, S. 1986, *Comments Astrophys.*, 11,151
- Tuohy, I. R., Garmire, G. P., Manchester, R. N. & Dopita, M. A. 1983, *ApJ*, 268, 778
- Umeda, H., Nomoto, K., Tsuruta, S., Muto, T. & Tatsumi, T. 1992, in *The Structure and Evolution of Neutron Stars*, ed. D. Pines, R. Tamagaki & S. Tsuruta (New York: Addison-Wesley) 406
- Umeda, H., Shibazaki, N., Nomoto, K. & Tsuruta, S. 1993, *ApJ*, 408, 186
- Van Riper, K. A. 1988, *ApJ*, 329, 339
- Van Riper, K. A. 1991, *ApJS*, 75, 449
- Wambach, J., Ainsworth, T. L. & Pines, D. 1991, in *Neutron Stars : Theory and Observation*, ed. J. Ventura & D. Pines (Dordrecht: Kluwer) 37
- Wiringa, R. B., Fiks, V. & Fabrocini, A. 1988, *Phys. Rev.*, C38, 1010

Fig. 1.— a) Proton 1S_0 pairing critical temperatures. CCY-Chao, Clark & Yang (1972), T73-Takatsuka (1973), NS-Niskanen & Sauls (1981), AO-Amundsen & Østgaard (1985a), WAP-Wambach *et al.* (1991).

b) Neutron 3P_2 pairing critical temperatures. HGRR-Hoffberg *et al.* (1970), T72-Takatsuka (1972), AO-Amundsen & Østgaard (1985b). The two dashed curves show the results of T72 and AO when the neutron effective mass is fixed at the free mass value.

In abscissa is the Fermi wave number k_F , related to the particle number density n_i by $k_F(n_i) = (3\pi^2 n_i)^{1/3} = 1.68(n_i/n_0)^{1/3}\text{fm}^{-1}$ where $n_0 = 0.16\text{fm}^{-3}$.

Fig. 2.— Cooling by the modified Urca process: effect of the specific heat suppression by nucleon pairing. The various curves correspond to the five EOSs we use: FP (continuous), WFF(av14) (dashed), MPA (dotted), PAL32 (dash-dotted) and PAL33 (dash-triple-dotted). $1.4 M_\odot$ star.

a) No core pairing at all.

b) Protons paired with a density-independent $T_c = 2 \times 10^9$ K.

c) Core neutrons paired with a density-independent $T_c = 2 \times 10^9$ K.

d) Protons and core neutrons paired with a density-independent $T_c = 2 \times 10^9$ K. Crust neutrons are paired according to Ainsworth *et al.* (1989). The temperature in ordinate is the effective temperature “at infinity,” i.e., redshifted. The cross shows Geminga’s temperature and age.

Fig. 3.— Cooling by the modified Urca process: effect of the star mass. EOS WFF(av14) and star mass of $1.2 M_\odot$ (dash-dotted), $1.4 M_\odot$ (continuous), $1.6 M_\odot$ (dash-triple dotted) and $1.8 M_\odot$ (dashed) with the same pairings as in Fig. 2. Crust neutrons are paired according to Ainsworth *et al.* (1989). The temperature in ordinate is the effective temperature “at infinity,” i.e., redshifted. The cross shows Geminga’s temperature and age.

Fig. 4.— Cooling by the modified Urca process: density dependent T_c . EOS WFF(av14) and star mass $1.4 M_\odot$. The continuous curve has no core neutron pairing, the other three curves have core neutron pairing as labeled (see Figure 1b). Core protons are not paired. Crust neutrons are paired according to Ainsworth *et al.* (1989). The temperature in ordinate is the effective temperature “at infinity,” i.e., redshifted. The cross shows Geminga’s temperature and age.

Fig. 5.— Fast neutrino cooling is not fast cooling forever: the curves show the cooling history of two neutron stars of very different masses built with the same EOS, WFF(av14), and the same pairings (HGRR for core neutrons, CCY-PSi) for core protons, as labeled in Figure 1, and Ainsworth *et al.* 1989 for crust neutrons). With this choice of pairings, neutrons are paired in the whole core for both stars, as are protons in the lighter star while the heavier star has a central region of unpaired protons. We have assumed that a kaon condensate develops above a density of 10^{15} gm/cm^3 such that the $1.6 M_{\odot}$ star has a kaon “pit” of $0.56 M_{\odot}$ while the $1.0 M_{\odot}$ star undergoes “standard” cooling. During the neutrino cooling era ($30 \text{ yr} < \text{age} < 3 \times 10^4 \text{ yr}$) the lighter star is warmer because of its low neutrino emission, while during the photon cooling era the heavier star is warmer because of its larger specific heat provided by its unpaired protons.

Fig. 6.— Comparison of the estimated surface temperatures of PSR 0656+14 and PSR 1055-52 with theoretical curves of slow neutrino cooling. EOS WFF(av14) and star mass $1.4 M_{\odot}$, no pairing (continuous), protons paired (dotted), neutrons paired (dash-dotted), neutrons and protons paired (dash-triple-dotted). The three temperatures for PSR 0656+14 correspond to blackbody, magnetic hydrogen, and nonmagnetic helium atmospheres as indicated, while the PSR 1055-52 temperature is from a blackbody fit. The age ranges correspond to braking indices from 2 to 4, as we used for Geminga, the upper values probably being overestimates.

Author Address

Dany Page: Instituto de Astronomía, U.N.A.M.,
Apdo postal 70-264, 04510 MEXICO D.F.

E-mail : PAGE@ASTROSCU.UNAM.MX

Figure 1

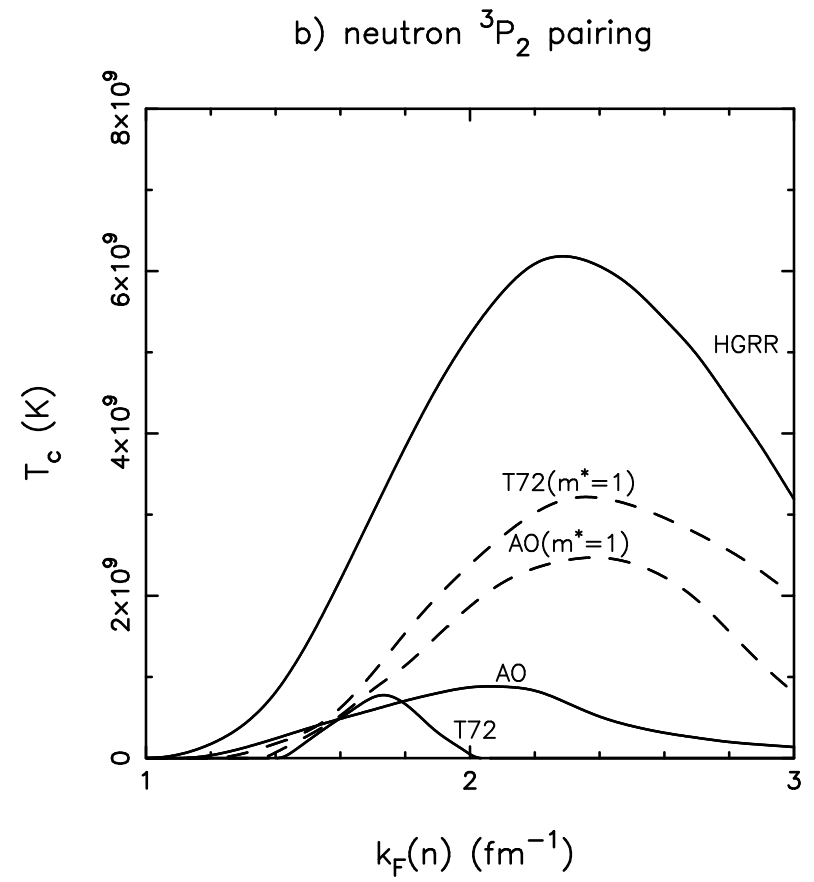
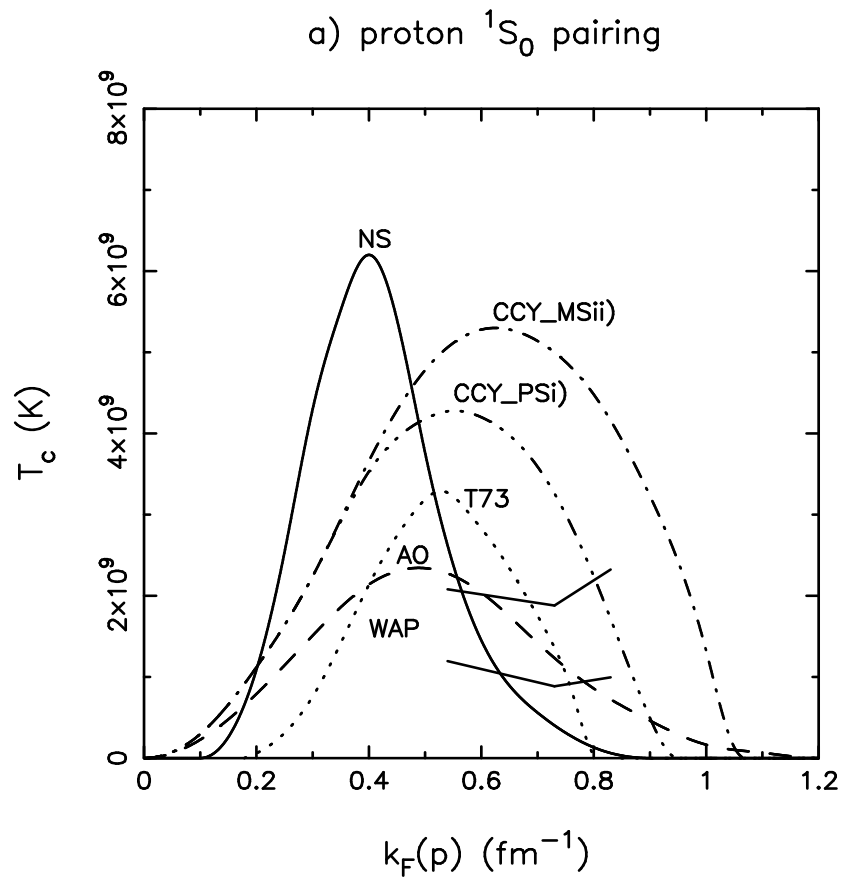


Figure 2

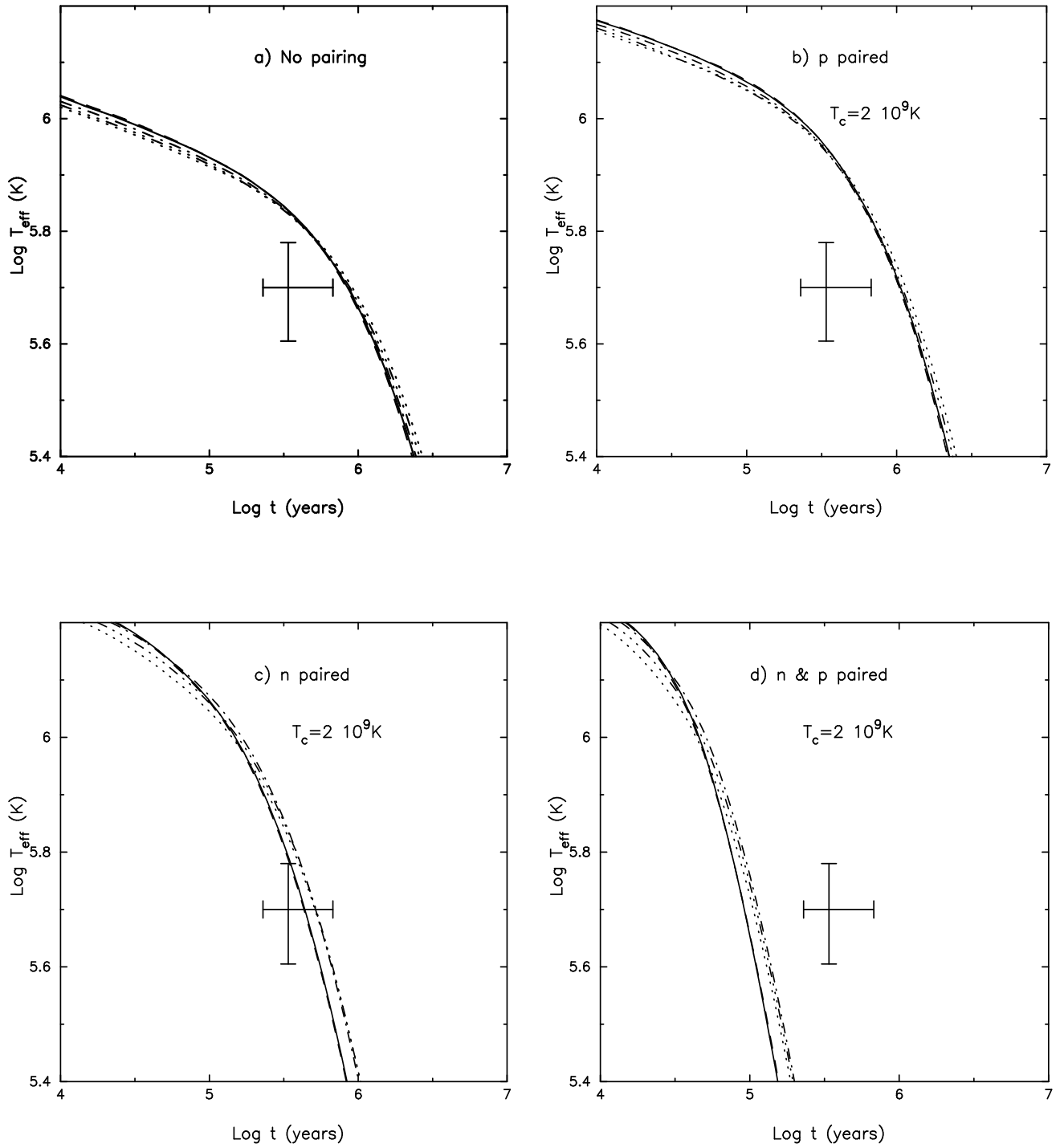


Figure 3

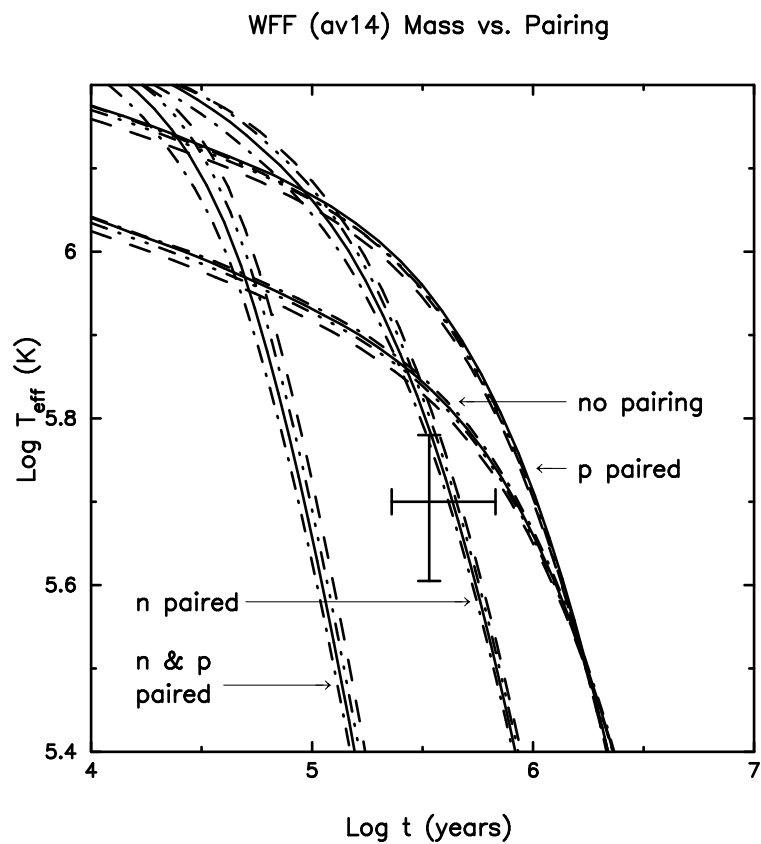


Figure 4

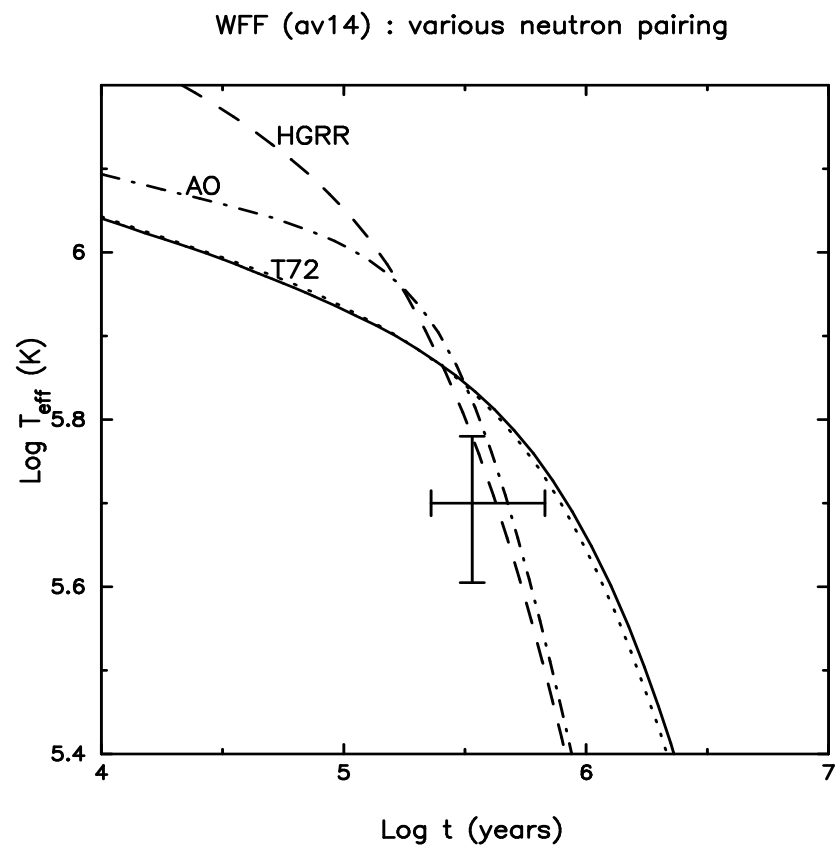


Figure 5

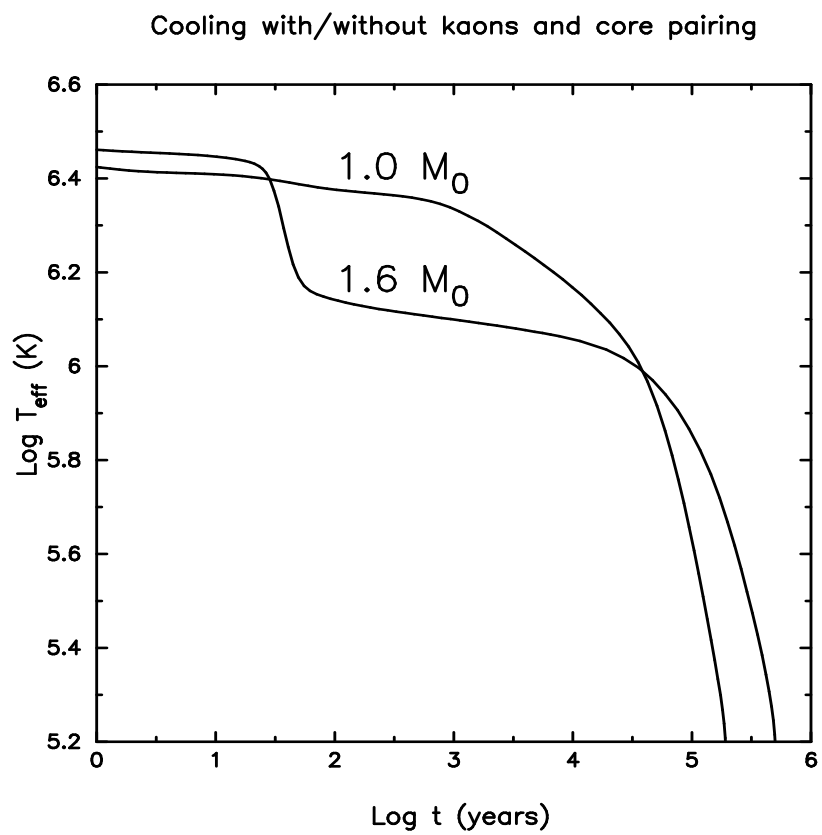


Figure 6

